

# Characterization of glucose transport mutants of *Saccharomyces cerevisiae* during a nutritional upshift reveals a correlation between metabolite levels and glycolytic flux

Daniel Bosch<sup>1</sup>, Mikael Johansson<sup>2</sup>, Cecilia Ferndahl<sup>1</sup>, Carl Johan Franzén<sup>2</sup>, Christer Larsson<sup>1</sup> & Lena Gustafsson<sup>1</sup>

<sup>1</sup>Molecular Biotechnology and <sup>2</sup>Chemical Reaction Engineering, Department of Chemical and Biological Engineering, Chalmers University of Technology, Göteborg, Sweden

**Correspondence:** Daniel Bosch, Department of Chemical and Biological Engineering, Molecular Biotechnology, Chalmers University of Technology, Box 462, SE-40530, Göteborg, Sweden. Tel.: +46 317 862 851; fax: +46 317 862 599; e-mail: daniel.bosch@gu.se

Received 23 February 2007; revised 21 August 2007; accepted 7 September 2007.  
First published online 27 November 2007.

DOI:10.1111/j.1567-1364.2007.00323.x

Editor: Barbara M. Bakker

## Keywords

sugar uptake; phosphofructokinase; hexose transporter; TM6\*

## Abstract

*Saccharomyces cerevisiae* shows a marked preference for glucose and fructose, revealed by the repression of genes whose products are involved in processing other carbon sources. This response seems to be driven by sugar phosphorylation in the first steps of glycolysis rather than by the external sugar concentration. To gain a further insight into the role of the internal sugar signalling mechanisms, we measured the levels of upper intracellular glycolytic metabolites and adenine nucleotides in three mutant strains, HXT1, HXT7 and TM6\*, with progressively reduced uptake capacities in comparison with the wild type. Reducing the rate of sugar consumption caused an accumulation of hexose phosphates upstream of the phosphofructokinase (PFK) and a reduction of fructose-1,6-bisphosphate levels. Mathematical modelling showed that these effects may be explained by changes in the kinetics of PFK and phosphoglucose isomerase. Moreover, the model indicated a modified sensitivity of the pyruvate dehydrogenase and the trichloroacetic acid cycle enzymes towards the NAD/NADH in the TM6\* strain. The activation of the SNF1 sugar signalling pathway, previously observed in the TM6\* strain, does not correlate with a reduction of the ATP:AMP ratio as reported in mammals. The mechanisms that may control the glycolytic rate at reduced sugar transport rates are discussed.

## Introduction

The monosaccharides glucose and fructose are the preferred carbon sources for most prokaryotic and eukaryotic cells. In nature, organisms have developed a number of mechanisms to secure a steady supply of these sugars in response to abrupt changes in their concentration. In the case of baker's yeast, *Saccharomyces cerevisiae*, glucose and fructose are incorporated by facilitated diffusion mediated by the hexose transporter family (Hxtp) (Boles & Hollenberg, 1997). This comprises at least 20 proteins with elevated sequence similarity and different sugar affinities and expression levels (Özcan & Johnston, 1999).

We have previously constructed and described a number of strains expressing different functional chimeras of the hexose transporters with a wide range of glucose uptake rates (Elbing *et al.*, 2004a). HXT1, HXT7 and TM6\* were

constructed by integrating a single hexose transporter gene (*HXT1*, *HXT7* and *TM6\**, respectively) into the genome of the *hxt* null strain KOY.VW100P (Elbing *et al.*, 2004a,b; Otterstedt *et al.*, 2004), which lacks all known hexose transporters and is unable to take up glucose (Wieczorke *et al.*, 1999). The hexose transporters were expressed under a truncated, strong and constitutive promoter. The difference in hexose transporters resulted in strains with different sugar consumption rates.

TM6\*p is a functional chimera composed of parts of the Hxt1p and Hxt7p transporters. In previous studies, it has been shown that the TM6\* strain is capable of maintaining respiratory growth even in the presence of high glucose concentrations while producing negligible amounts of ethanol (Otterstedt *et al.*, 2004). This is in contrast to wild-type strains of *S. cerevisiae*, which, under similar conditions, mainly ferment glucose into ethanol and carbon dioxide

(CO<sub>2</sub>) (Fiechter *et al.*, 1981; Verduyn *et al.*, 1984). The wild type can only attain the fully respiratory catabolism shown by the TM6\* strain when it is grown in glucose-limited chemostats or fed-batch reactors at low dilution rates (Postma *et al.*, 1989).

The addition of glucose or fructose to wild-type cells growing on a respiratory carbon source leads to major changes in gene expression. A large set of genes becomes repressed, for example, those implicated in the trichloroacetic acid (TCA) cycle, glyoxylate cycle, the respiratory chain and the uptake and utilization of alternative carbon sources (Ronne, 1995; Gancedo, 1998; Carlson, 1999). After depletion of glucose or fructose, e.g. at the diauxic shift, repression is relieved (DeRisi *et al.*, 1997). Studies on the transcription pattern of the TM6\* strain revealed that even at high glucose concentrations, the profile is very similar to that of the wild type in the absence of sugars (Elbing *et al.*, 2004a, b). This piece of evidence indicates that external levels of glucose do not control the metabolic switch from fermentation to respiration. Presumably, there is an intracellular signal leading to glucose repression, but its identity remains unknown. A number of potential candidates have been proposed, for instance Hxk2 (Rose *et al.*, 1991; De Winde *et al.*, 1996; Hohmann *et al.*, 1999; Rolland *et al.*, 2002), cAMP (Rolland *et al.*, 2001), the concentration of selected intracellular metabolites (Boles & Zimmermann, 1993; Boles *et al.*, 1993) and the ATP:AMP ratio (Wilson *et al.*, 1996). This signal may also control glycolytic flux by influencing the kinetics of one or several enzymes in the route; for instance, modifying the allosteric regulation of hexokinase (HK), phosphofructokinase (PFK) and pyruvate kinase (PK) (Gancedo, 1998) or the regulation of enzymes at the end of phosphorylation cascades, e.g. 6-phosphofructo-2-kinase (Pfk2) by MAPK (Dihazi *et al.*, 2004) and fructose-2, 6-bisphosphatase (Fbp26) by cAMP (Boles *et al.*, 1997). Moreover, some glycolytic- and ethanol-producing enzymes have been revealed as regulators of transcriptional activity e.g. Hxk2 (de la Cera *et al.*, 2002) and Pdc1 (Mojžita, 2007) in yeast, and Hxk1 in *Arabidopsis thaliana* (Cho *et al.*, 2006).

In this study, we address how a reduction in sugar uptake leads to a slow glycolytic rate, therefore causing the shift from respiration to fermentation. We show that the intracellular levels of glycolytic metabolites and adenosine nucleotides are very different in strains with high sugar consumption rates, i.e. the wild type and HXT1 strains, in comparison with strains exhibiting low sugar consumption rates, i.e. HXT7 and TM6\*, at the same external sugar concentration. Furthermore, mathematical modelling of the glycolytic flux suggests that these observations may be explained by differences in the kinetics of the PFK and phosphoglucose isomerase (PGI), and by a modified sensitivity of the pyruvate dehydrogenase (PDH) and/or the TCA cycle enzymes towards NAD<sup>+</sup> and NADH.

## Materials and methods

### Strains

All *S. cerevisiae* strains used were derived from the CEN.PK2-1C strain (van Dijken *et al.*, 2000), herein referred to as the wild type. The construction of the prototrophic strains KOY.HXT1P (HXT1), KOY.HXT7P (HXT7) and KOY.TM6\*P (TM6\*) has been described by Elbing *et al.* (2004a).

### Growth conditions

An aerobic chemostat culture with a working volume of 2 L and a constant dilution rate of 0.1 h<sup>-1</sup> was prepared in a Braun Biostat A fermentor (Braun, Melsungen, Germany). In all cultivations, a two-times concentrated defined minimal medium was used (Verduyn *et al.*, 1992). An antifoaming agent (Polypropylene-2000 Fluka, Steinheim, Switzerland) was added to a final concentration of 0.1 mL L<sup>-1</sup> in the bioreactors. The temperature was maintained constant at 30 °C, and the stirring rate was 1200 r.p.m. The pH was kept at 5.0 by the automatic addition of 1 M NaOH. The airflow was controlled by a mass flow controller from Bronkhorst, High-Tech, B.V. (Ruurlo, the Netherlands). Cells were precultured overnight in defined medium with 2% (110 mM) glucose as the sole carbon source. The preculture was subsequently used to inoculate a 2 L fermentor with 5% glucose. The feed of fresh substrate with 1% of ethanol as the sole carbon source was started following glucose depletion, as indicated by the CO<sub>2</sub> production rate. Once the chemostat culture achieved a constant CO<sub>2</sub> production for at least three volume changes, sugar was pulsed into the vessel, enough to bring the transient concentration to 2%. Simultaneously, the ethanol medium feed was shut off. Oxygen consumption and CO<sub>2</sub> production rate were followed online using a photoacoustic gas analyser (type 1308; Brüel and Kjær, Nærum, Denmark).

### Dry weight determination

Dry weight was measured in triplicate by centrifugation of 3 × 10 mL of cell culture in preweighed dry glass tubes. The cells were washed twice in 5 mL of deionized water (MilliQ), dried for 24 h at 110 °C and stored in a desiccator before weighing.

### Determination of extracellular substrate and products

Duplicate samples of 1 mL each were sterile filtered (0.22 µm), frozen in liquid N<sub>2</sub> and stored at -20 °C. The analyses of glucose, ethanol and glycerol were performed using enzymatic combination kits (Boehringer-Mannheim GmbH, Mannheim, Germany).

### Consumption and production rates

The mean rates of glucose and fructose consumption and ethanol production were determined for the 2-h interval subsequent to sugar addition. The mean values of the dry weight in the specified time intervals were used in the rate calculations.

### Determination of glycogen and trehalose

Duplicate samples of 5 mL were centrifuged at 4 °C and the pellets were frozen in liquid nitrogen, maintained at -40 °C and analysed as described previously (Parrou & François, 1997). The content of storage carbohydrates was normalized to the cell dry weight of the same culture samples.

### Determination of intracellular metabolites

For all metabolites, except ATP, six samples of 3 mL each were directly transferred into preweighed tubes with 10 mL of methanol maintained at -48 °C; the final concentration of methanol (v/v) was about 75%. The extraction was performed as described previously (Gustafsson, 1979). The extraction and quantification of ATP was performed separately. Triplicate samples of 1 mL each were added to 1.2 mL of 0.51 M TCA, thereby extracting ATP as described earlier in Gustafsson (1979). The ATP concentration was analysed in triplicate on a Packard Pico-Lite luminometer (Packard Instruments, Downers Grove, IL) using ATP bioluminescence assay kits (CLSII) (Roche Diagnostics, Mannheim, Germany).

### Measurement of sugar uptake capacity

Samples for determination of the sugar uptake were taken during steady-state growth on ethanol. Cells were harvested and washed twice with 0.1 M potassium phosphate buffer (pH 6.5), diluted to a cell density of 75 g L<sup>-1</sup> (wet weight) and kept on ice. Uptake of [<sup>14</sup>C] glucose (Amersham Life Science, Uppsala, Sweden) was assayed as described by Özcan *et al.* (1993) with the modifications developed by Walsh *et al.* (1994). Radioactivity was quantified using a liquid scintillation detector (Beckman Coulter AB, Bromma, Sweden). Total cellular protein was determined with the bichloroacetic acid kit (Bio-Rad Laboratories Inc., Hercules, CA). Three separate series at seven different sugar concentrations were performed. Data were analysed using Hanes plots.

### Mathematical modelling

A kinetic model was constructed to describe respiro-fermentative growth on glucose during the 2-h transients after the glucose pulse to the four strains. The stoichiometry and kinetic rate equations of the reaction network are shown in Table 1. F16BP was not included in the model, because it is known that yeast cells adapted to grow on ethanol and

subjected to a sugar pulse degrade F16BP and synthesize PFK very rapidly, making the switch instantaneous in this time scale (Regelmann *et al.*, 2003).

Polynomial approximations of the glucose uptake rate, the oxygen uptake rate and the biomass concentration were used as input to the model. Biosynthesis was described as a lumped reaction from several glycolytic intermediates. It was adapted from the aerobic case described by Sárvári Horváth *et al.* (2003). The average macromolecular composition of cells was assumed to be 50% (w/w) protein (average amino acid composition according to Albers *et al.*, 1996), 10% RNA (average nucleotide composition according to Mounolou, 1975), 30% carbohydrates, 5% lipids and 5% ash. The intracellular AMP concentration was set as the average of the measured values for each time course. The total pool of ATP and ADP was set equal to the average sum during each time course. The total NAD<sup>+</sup>+NADH pool was set to 3 mM, with the exception of the HXT1 strain, for which it was set to 3.4 mM, corresponding to the same ratio between the assumed total pool and the measured initial NAD<sup>+</sup> concentration as in the wild type. The errors between the measured and predicted intracellular concentrations of G6P, F6P, F16BP, pyruvate, ADP, ATP and NAD<sup>+</sup>, the extracellular concentrations of ethanol and glycerol and the CO<sub>2</sub> evolution rates were used for parameter optimization. The maximum rates ( $V_{\max}$  values) for PFK, aldolase, GapDH, Lp-PEP, PK, PDC, ADH, Lp-GDP and Lp-ATP were optimized. For Lp-PDH and complete TCA cycle reactions,  $V_{\max}$  as well as  $K_{\text{NAD}}$  and  $K_{\text{I,NADH}}$  were fitted.

The increase in expression during the pulse was taken into consideration by fitting an expression factor for the upper part of glycolysis, and one for PDC, such that the  $V_{\max}$  values of these reactions were multiplied by a factor  $(1 + \text{Expr } t)$ . ADH and GapDH were assumed to be linearly expressed from zero to full expression during the 120 min of the pulse for the wild type and HXT1 strains, while constant expression gave a better fit for the HXT7 and the TM6\* strains. For the TM6\* strain,  $V_{\max}$  for phosphoglucose isomerase was also adjusted.

Parameters were estimated using the nonlinear least squares minimization function lsqnonlin.m and the stiff ordinary differential equation solver ode15s.m in MATLAB<sup>®</sup> 6.5. The parameter values were scaled with 10<sup>-5</sup> times the inverse of the initial values, to give a uniform parameter set for improved efficiency of the minimization routine. Owing to evaporation likely leading to erroneous ethanol measurements, ethanol was weighted by a factor 0.5 in the sum of squares, while glycerol was weighted by a factor 10. Global minimum cannot be 100% guaranteed, but the optimum was the best result from several different initial guesses for the parameter values. For the HXT7 and the TM6\* strains, this procedure unfortunately only produced infeasible results (negative F16BP, acetaldehyde, or ethanol

**Table 1.** Stoichiometry and kinetics of the reaction in the kinetic model

Rate equation	Parameter values
<p><i>Glucose transport</i></p> $\text{Glc}_x \rightarrow \text{Glc}$ $V_{\text{GlcTransp}}$	$V_{\text{GlcTransp}} = \text{measured}$
<p><i>Hexokinase</i></p> $\text{Glc} + \text{ATP} \rightarrow \text{G6P} + \text{ADP}$ $V_{\text{HK}} = (1 + \text{Expr}_1 t) \frac{V_{3m} [\text{Glc}] [\text{ATP}]}{K_{3\text{DGlC}} K_{3\text{ATP}} + K_{3\text{GlC}} [\text{ATP}] + K_{3\text{ATP}} [\text{Glc}] + [\text{Glc}] [\text{ATP}]}$	<p>Hynne <i>et al.</i> (2001)  <math>V_{3m} = 1000 \text{ mM min}^{-1}</math> (est)</p> <p><math>K_{3\text{ATP}} = 0.1 \text{ mM}</math>  <math>K_{3\text{GlC}} = 0 \text{ mM}</math>  <math>K_{3\text{DGlC}} = 0.37 \text{ mM}</math></p>
<p><i>Phosphoglucose isomerase</i></p> $\text{G6P} \leftrightarrow \text{F6P}$ $V_{\text{PGI}} = (1 + \text{Expr}_1 t) \frac{V_{4m} \left[ [\text{G6P}] - \frac{[\text{F6P}]}{K_{4\text{eq}}} \right]}{K_{4\text{G6P}} + [\text{G6P}] + \frac{K_{4\text{G6P}}}{K_{4\text{F6P}}} [\text{F6P}]}$	<p>Hynne <i>et al.</i> (2001)  <math>V_{4m} = \text{estimated}</math></p> <p><math>K_{4\text{G6P}} = 0.8 \text{ mM}</math>  <math>K_{4\text{G6P}} = 0.15 \text{ mM}</math>  <math>K_{4\text{eq}} = 0.30 \text{ mM}</math>  <math>\text{Expr}_1 = \text{estimated}</math></p>
<p><i>Phosphofructokinase</i></p> $\text{F6P} + \text{ATP} \rightarrow \text{F16BP} + \text{ADP}$ $V_{\text{PFK}} = (1 + \text{Expr}_1 t) \frac{V_{5m} g_R \lambda_1 \lambda_2 (1 + \lambda_1 \lambda_2 + g_R \lambda_1 \lambda_2)}{(1 + \lambda_1 \lambda_2 + g_R \lambda_1 \lambda_2)^2 + L (1 + c_{\text{ATP}} \lambda_2)^2}$ $\lambda_1 = \frac{[\text{F6P}]}{K_{R, \text{F6P}}}; \quad \lambda_2 = \frac{[\text{ATP}]}{K_{R, \text{ATP}}}$	<p>Teusink <i>et al.</i> (2000)  <math>V_{5m} = \text{estimated}</math></p> <p><math>K_{\text{ATP}} = 0.65 \text{ mM}</math>  <math>K_{\text{AMP}} = 0.0995 \text{ mM}</math>  <math>K_{R, \text{ATP}} = 0.71 \text{ mM}</math>  <math>\text{Expr}_1 = \text{estimated}</math></p> <p><math>K_{R, \text{F6P}} = 0.1 \text{ mM}</math>  <math>K_{\text{F26BP}} = 0.000682 \text{ mM}</math></p>
$L = L_0 \left[ \frac{1 + c_{i, \text{ATP}} [\text{ATP}] / K_{\text{ATP}}}{1 + [\text{ATP}] / K_{\text{ATP}}} \right]^2 \left[ \frac{1 + c_{i, \text{AMP}} [\text{AMP}] / K_{\text{AMP}}}{1 + [\text{AMP}] / K_{\text{AMP}}} \right]^2 \left[ \frac{1 + c_{i, \text{F26BP}} [\text{F26BP}] / K_{\text{F26BP}} + c_{i, \text{F16BP}} [\text{F16BP}] / K_{\text{F16BP}}}{1 + [\text{F26BP}] / K_{\text{F26BP}} + [\text{F16BP}] / K_{\text{F16BP}}} \right]^2$	<p><math>K_{\text{F16BP}} = 0.111 \text{ mM}</math>  <math>c_{\text{ATP}} = 3</math>  <math>c_{i, \text{ATP}} = 100</math>  <math>c_{i, \text{AMP}} = 0.0845</math>  <math>c_{i, \text{F26BP}} = 0.0174</math>  <math>c_{i, \text{F16BP}} = 0.397</math>  <math>g_R = 5.12</math>  <math>L_0 = 0.66</math></p>
<p><i>Aldolase</i></p> $\text{F16bP} \leftrightarrow \text{DHAP} + \text{GAP}$ $V_{\text{ALD}} = \frac{(1 + \text{Expr}_1 t) V_{6m} \left[ [\text{F16bP}] - \frac{5[\text{GAP}][\text{DHAP}]}{K_{5\text{eq}}} \right]}{\left( K_{6\text{F16bP}} + [\text{F16bP}] + \frac{[\text{GAP}] K_{6\text{DHAP}} 5}{K_{6\text{eq}}} + \frac{[\text{DHAP}] K_{6\text{GAP}} 5}{K_{6\text{eq}}} \right) \left( \frac{[\text{F16bP}][\text{GAP}]}{K_{6\text{IGAP}}} + \frac{[\text{GAP}][\text{DHAP}] 5}{K_{6\text{eq}}} \right)}$	<p>Hynne <i>et al.</i> (2001)  <math>V_{6m} = \text{estimated}</math></p> <p><math>K_{6\text{F16bP}} = 0.3 \text{ mM}</math>  <math>K_{6\text{DHAP}} = 2.0 \text{ mM}</math>  <math>K_{6\text{GAP}} = 4.0 \text{ mM}</math>  <math>K_{6\text{IGAP}} = 10.0 \text{ mM}</math>  <math>K_{6\text{eq}} = 0.081 \text{ mM}</math>  <math>\text{Expr}_1 = \text{estimated}</math></p>

Table 1. Continued.

Rate equation	Parameter values
<p><i>Triosephosphate isomerase</i></p> $\text{DHAP} \leftrightarrow \text{GAP}$ $V_{\text{TIM}} = \frac{V_{7m} \left[ \text{DHAP} - \frac{[\text{GAP}]}{K_{7\text{eq}}} \right]}{K_{7\text{DHAP}} + [\text{DHAP}] + \frac{K_{7\text{DHAP}}[\text{GAP}]}{K_{7\text{GAP}}}}$	<p>Hynne et al. (2001)</p> <p><math>V_{7m} = 116.4 \text{ mM min}^{-1}</math></p> <p><math>K_{7\text{DHAP}} = 1.23 \text{ mM}</math>  <math>K_{7\text{GAP}} = 1.27 \text{ mM}</math>  <math>K_{7\text{eq}} = 0.045 \text{ mM}</math></p>
<p><i>Glyceraldehyde-3-phosphate dehydrogenase</i></p> $\text{GAP} + \text{NAD}^+ \leftrightarrow \text{BPG} + \text{NADH} + \text{H}^+$ $V_{\text{GAPDH}} = (1 + \text{Expr}_1 t) \frac{V_{8m} \left[ \frac{[\text{GAP}][\text{NAD}][\text{BPG}][\text{NADH}]}{K_{8\text{eq}}} \right]}{K_{8\text{GAP}} K_{8\text{NAD}} \left[ 1 + \frac{[\text{GAP}]}{K_{8\text{GAP}}} + \frac{[\text{BPG}]}{K_{8\text{BPG}}} \right] \left[ 1 + \frac{[\text{NAD}]}{K_{8\text{NAD}}} + \frac{[\text{NADH}]}{K_{8\text{NADH}}} \right]}$	<p>Hynne et al. (2001)</p> <p><math>V_{8m}</math> = estimated</p> <p><math>K_{8\text{GAP}} = 0.6 \text{ mM}</math>  <math>K_{8\text{BPG}} = 0.01 \text{ mM}</math>  <math>K_{8\text{NAD}} = 0.1 \text{ mM}</math>  <math>K_{8\text{NADH}} = 0.06 \text{ mM}</math>  <math>K_{8\text{eq}} = 0.0055</math>  <math>\text{Expr}_1</math> = estimated</p>
<p><i>Lp-PGK, Lumped reactions from BPG to PEP</i></p> $\text{BPG} + \text{ADP} + \text{P}_i \leftrightarrow \text{PEP} + \text{ATP}$ $V_{\text{PEP}} = k_{9f}[\text{BPG}][\text{ADP}] - k_{9r}[\text{PEP}][\text{ATP}]$	<p>Hynne et al. (2001)</p> <p><math>k_{9f} = 4.44 \times 10^5 \text{ min}^{-1}</math></p> <p><math>k_{9r} = 1530 \text{ min}^{-1}</math></p>
<p><i>Pyruvate kinase</i></p> $\text{PEP} + \text{ADP} + \text{P}_i \rightarrow \text{PYR} + \text{ATP}$ $V_{\text{PK}} = \frac{V_{10m} \frac{[\text{PEP}]}{K_{\text{PEP}10}} \left[ \frac{[\text{PEP}]}{K_{\text{PEP}10}} + 1 \right]^{(n_{10}-1)}}{L_{0,10} \left[ \frac{[\text{ATP}] + 1}{\frac{K_{\text{ATP}10}}{[\text{F16bP}] + 1}} + 1 \right]^{n_{10}} + \left[ 1 + \frac{[\text{PEP}]}{K_{\text{PEP}10}} \right]^{n_{10}}} \frac{[\text{ADP}]}{[\text{ADP}] + K_{\text{ADP}10}}$	<p>Rizzi et al. (1997), Johannes &amp; Hess (1973)</p> <p><math>V_{10m}</math> = estimated</p> <p><math>K_{\text{PEP}10} = 0.19 \text{ mM}</math>  <math>K_{\text{ATP}10} = 9.3 \text{ mM}</math>  <math>K_{\text{FBP}10} = 0.2 \text{ mM}</math>  <math>K_{\text{ADP}10} = 0.3 \text{ mM}</math>  <math>n_{10} = 4</math>  <math>L_{0,10} = 60\,000</math></p>
<p><i>Lp-PDH, Lumped reactions from pyruvate to the complete TCA</i></p> $\text{PYR} + 5 \text{NAD}^+ + \text{ADP} + \text{P}_i \rightarrow 3 \text{CO}_2 + 5 \text{NADH} + 5 \text{H}^+ + \text{ATP}$ $V_{\text{TCA}} = \frac{V_{\text{PDH}}[\text{PYR}][\text{NAD}]}{\left( K_{\text{NAD}13}[\text{PYR}] + K_{\text{PYR}13}[\text{NAD}] + \frac{K_{\text{I-PYR}13} K_{\text{NAD}13}[\text{NADH}]}{K_{\text{I-NADH}13}} \right) + [\text{PYR}][\text{NAD}] + \frac{K_{\text{NAD}13}[\text{PYR}][\text{NADH}]}{K_{\text{I-NADH}13}}}$	<p>Rizzi et al. (1997)</p> <p><math>V_{\text{PDH}}</math> = estimated</p> <p><math>K_{\text{NAD}13}</math> = estimated  <math>K_{\text{I-NADH}13}</math> = estimated  <math>K_{\text{PYR}13} = 70 \text{ mM}</math>  <math>K_{\text{I-PYR}13} = 20 \text{ mM}</math></p>
<p><i>Pyruvate decarboxylase</i></p> $\text{PYR} \rightarrow \text{ACA} + \text{CO}_2$ $V_{\text{PDC}} = (1 + \text{Expr}_2 t) \frac{V_{11m} \left[ \frac{[\text{PYR}]}{K_{11}} \right]^{n_{11}}}{1 + \left[ \frac{[\text{PYR}]}{K_{11}} \right]^{n_{11}}}$	<p>Teusink et al. (2000)</p> <p><math>V_{11m}</math> = estimated</p> <p><math>K_{11} = 4.3 \text{ mM}</math>  <math>n_{11} = 1.9</math>  <math>\text{Expr}_2</math> = estimated</p>

**Table 1.** Continued.

Rate equation	Parameter values
<p>Alcohol dehydrogenase (<i>ADH1</i>)</p> $\text{ACA} + \text{NADH} + \text{H}^+ \leftrightarrow \text{EtOH} + \text{NAD}^+$ $V_{\text{ADH}} = \frac{K_t V_{12m} \left( \frac{[\text{ACA}][\text{NADH}]}{K_{\text{INADH}}K_{\text{ACA}}} - \frac{[\text{EtOH}][\text{NAD}]}{K_{\text{IEtOH}}K_{\text{NAD}}} \right)}{\left( 1 + \frac{[\text{EtOH}]}{K_{\text{IEtOH}}} + \frac{K_{\text{EtOH}}[\text{NAD}]}{K_{\text{IEtOH}}K_{\text{NAD}}} + \frac{K_{\text{NADH}}[\text{ACA}]}{K_{\text{INADH}}K_{\text{ACA}}} + \frac{[\text{NADH}]}{K_{\text{INADH}}} \right.}$ $\left. + \frac{[\text{EtOH}][\text{NAD}]}{K_{\text{NAD}}K_{\text{IEtOH}}} + \frac{K_{\text{NADH}}[\text{EtOH}][\text{ACA}]}{K_{\text{IEtOH}}K_{\text{INADH}}K_{\text{ACA}}} + \frac{K_{\text{EtOH}}[\text{NAD}][\text{NADH}]}{K_{\text{NAD}}K_{\text{IEtOH}}K_{\text{INADH}}} \right.}$ $\left. + \frac{[\text{ACA}][\text{NADH}]}{K_{\text{ACA}}K_{\text{INADH}}} + \frac{[\text{EtOH}][\text{NAD}][\text{ACA}]}{K_{\text{IEtOH}}K_{\text{NAD}}K_{\text{IACA}}} + \frac{[\text{NAD}][\text{ACA}][\text{NADH}]}{K_{\text{NAD}}K_{\text{IEtOH}}K_{\text{INADH}}} \right)$	<p>Ganzhorn <i>et al.</i> (1987), Teusink <i>et al.</i> (2000) <math>V_{12m}</math> = estimated <math>K_{\text{EtOH}} = 17 \text{ mM}</math></p> <p><math>K_{\text{IEtOH}} = 90 \text{ mM}</math> <math>K_{\text{ACA}} = 1.1 \text{ mM}</math> <math>K_{\text{IACA}} = 1.1 \text{ mM}</math> <math>K_{\text{NAD}} = 0.17 \text{ mM}</math> <math>K_{\text{INAD}} = 0.92 \text{ mM}</math> <math>K_{\text{NADH}} = 0.11 \text{ mM}</math> <math>K_{\text{INADH}} = 0.03 \text{ mM}</math> <math>K_t = t</math> for WT and HXT1, <math>K_t = 1</math> for HXT7 and TM6*</p>
<p><i>Lp-GPD</i> Lumped reactions from DHAP to glycerol</p> $\text{DHAP} + \text{NADH} + \text{H}^+ \rightarrow \text{Glyc} + \text{NAD}^+$ $V_{\text{pGLYC}} = \frac{K_t V_{15m} [\text{DHAP}]}{\left( K_{15\text{DHAP}} \left[ 1 + \frac{K_{15\text{INADH}}}{[\text{NADH}]} \left( 1 + \frac{[\text{NAD}]}{K_{15\text{INAD}}} \right) \right] \right.}$ $\left. + [\text{DHAP}] \left[ 1 + \frac{K_{15\text{NADH}}}{[\text{NADH}]} \left( 1 + \frac{[\text{NAD}]}{K_{15\text{INAD}}} \right) \right] \right)$	<p>Hynne <i>et al.</i> (2001) <math>V_{15m}</math> = estimated</p> <p><math>K_{15\text{DHAP}} = 25 \text{ mM}</math> <math>K_{15\text{INAD}} = 0.13 \text{ mM}</math> <math>K_{15\text{NADH}} = 0.034 \text{ mM}</math> <math>K_{15\text{INADH}} = 0.13 \text{ mM}</math> <math>K_t = t</math> for WT and HXT1, <math>K_t = 1</math> for HXT7 and TM6*</p>
<p>Diffusion of ethanol</p> $\text{EtOH} \leftrightarrow \text{EtOH}_e$ $V_{\text{diffEtOH}} = k_{13}([\text{EtOH}] - [\text{EtOH}_e])$	<p>Hynne <i>et al.</i> (2001) <math>k_{13} = 16.72 \text{ min}^{-1}</math></p>
<p>Diffusion of glycerol</p> $\text{Glyc} \leftrightarrow \text{Glyc}_e$ $V_{\text{diffGlyc}} = k_{16}([\text{Glyc}] - [\text{Glyc}_e])$	<p>Hynne <i>et al.</i> (2001) <math>k_{16} = 1.9 \text{ min}^{-1}</math></p>
<p>Oxygen consumption</p> $\text{NADH} + \text{H}^+ + \text{ADP} + \text{P}_i + 0.5\text{O}_2 \rightarrow \text{NAD}^+ + \text{ATP} + \text{H}_2\text{O}$ $V_{\text{resp}} = 2r_{\text{O}_2\text{uptake}} - 0.002658 v_{\text{biomass}}$	<p><math>r_{\text{O}_2\text{uptake}}</math> = measured</p>
<p><i>Lp-ATP</i> (Lumped nonspecific ATP consumption)</p> $\text{ATP} \rightarrow \text{ADP} + \text{P}_i$ $V_{\text{cons}} = k_{23}[\text{ATP}]$	<p>Hynne <i>et al.</i> (2001) <math>k_{23}</math> = estimated</p>

**Table 1.** Continued.

Rate equation	Parameter values
Biomass formation	Adapted from Sárvári Horváth et al. (2003) $V_{\text{Biomass}}$ = measured
$0.07520 \text{ G6P} + 0.02318 \text{ BPG} + 0.01551 \text{ PEP} + 0.11791 \text{ PYR} + 0.06624$ $\text{ACA} + 0.00118 \text{ GLYC} + 0.09194 \text{ NAD}^+ \rightarrow \text{Biomass} + 0.00776 \text{ F6P} + 0.00108$ $\text{GAP} + 0.09194 (\text{NADH} + \text{H}^+) + 0.00922 \text{ CO}_2 + 0.00266 \text{ O}_2$ $V_{\text{Biomass}}$	

concentrations, or massive accumulation of acetaldehyde or the hexose phosphates). Therefore, the parameter values for these strains were estimated by manual tuning.

The momentaneous biomass yield on ATP was calculated as the estimated growth rate [ $\text{g (L cell)}^{-1} \text{ min}^{-1}$ ] divided by the estimated ATP consumption rate [ $\text{mol (L cell)}^{-1} \text{ min}^{-1}$ ] at each time point.

## Results

### Sugar consumption rate correlated with product formation of four strains with different glycolytic flux

The four strains were cultured in chemostats with ethanol as the limiting substrate at a dilution rate of  $0.1 \text{ h}^{-1}$ . A constant  $\text{CO}_2$  production level for at least three volume changes indicated steady-state growth (Fig. 1). The inflow was stopped, and either glucose or fructose was added to a final concentration of 110 mM (2%), turning the continuous culture into a batch cultivation. The  $\text{CO}_2$  evolution varied for the four strains tested. In the wild type (Fig. 1a), sugar addition led to a sustained increase of  $\text{CO}_2$  production for the 2-h span of the experiment. In contrast, the gas production rate of the HXT1 strain (Fig. 1b) reached a plateau a few minutes after the sugar pulse and thereafter remained constant. The HXT7 strain (Fig. 1c) displayed a slow increase in  $\text{CO}_2$  over the 2 h studied. In the TM6\* strain, the  $\text{CO}_2$  profile was completely different, because it declined on sugar addition and subsequently stabilized on a reduced level (Fig. 1d).

The observed differences of the  $\text{CO}_2$  profiles are in line with the observed sugar consumption and production rates. Figure 2a illustrates that the sugar consumption was the largest for the wild type, followed by the HXT1 and HXT7 strains, which consumed about half of the sugar added within 2 h. The TM6\* strain showed a very low sugar consumption within the experimental time. These differences were further illustrated by the calculated sugar con-

sumption rates (Table 2). The mean sugar consumption rate was reduced in all the mutant strains compared with the wild type, which showed a glucose consumption rate of  $3.2 \text{ mmol glucose (g dry weight)}^{-1} \text{ h}^{-1}$ . The HXT1 strain showed a 25% reduction, the HXT7 strain a 50% reduction and the TM6\* strain a 90% reduction compared with the wild type.

Measurements of the sugar uptake capacity were made on steady-state cultivations fed with ethanol as the carbon source. The results were in the same range as the sugar consumption rates obtained during the pulse experiments. The  $V_{\text{max}}$  values ranged from 0.9 to  $1.8 \text{ mmol glucose (g dry weight)}^{-1} \text{ h}^{-1}$  and  $1.7\text{--}3.9 \text{ mmol fructose (g dry weight)}^{-1} \text{ h}^{-1}$ , but there were no systematic differences between the uptake capacities of the different strains.

Ethanol is the main product of yeast fermentation and there were clear differences in ethanol production for the four strains analysed (Fig. 2b). While the wild-type strain produced large quantities of ethanol, up to 70 mM during the 2 h of measurement, the production of the HXT1 strain did not exceed 30 mM. Yet, the most astonishing result was that the HXT7 strain did not produce noticeable amounts of ethanol even though the sugar consumption rate was five times higher than that of the TM6\* strain, which, as expected, did not generate any detectable ethanol. Glycerol, which is a common by-product during fermentation, was also measured (Fig. 2c). The wild-type strain did not start releasing glycerol until 30 min after sugar addition. On the other hand, the HXT1 strain produced glycerol continuously and so did the HXT7 strain, albeit in smaller amounts. The glycerol production should be especially noticed because this strain did not produce any ethanol. The TM6\* strain generated barely detectable amounts of glycerol.

The behaviour of the studied strains in medium containing either glucose or fructose did not show large disparities. Both sugars were consumed similarly; however, some differences in the ethanol released were apparent for wild type and HXT1 strains, the latter also showed differences in glycerol

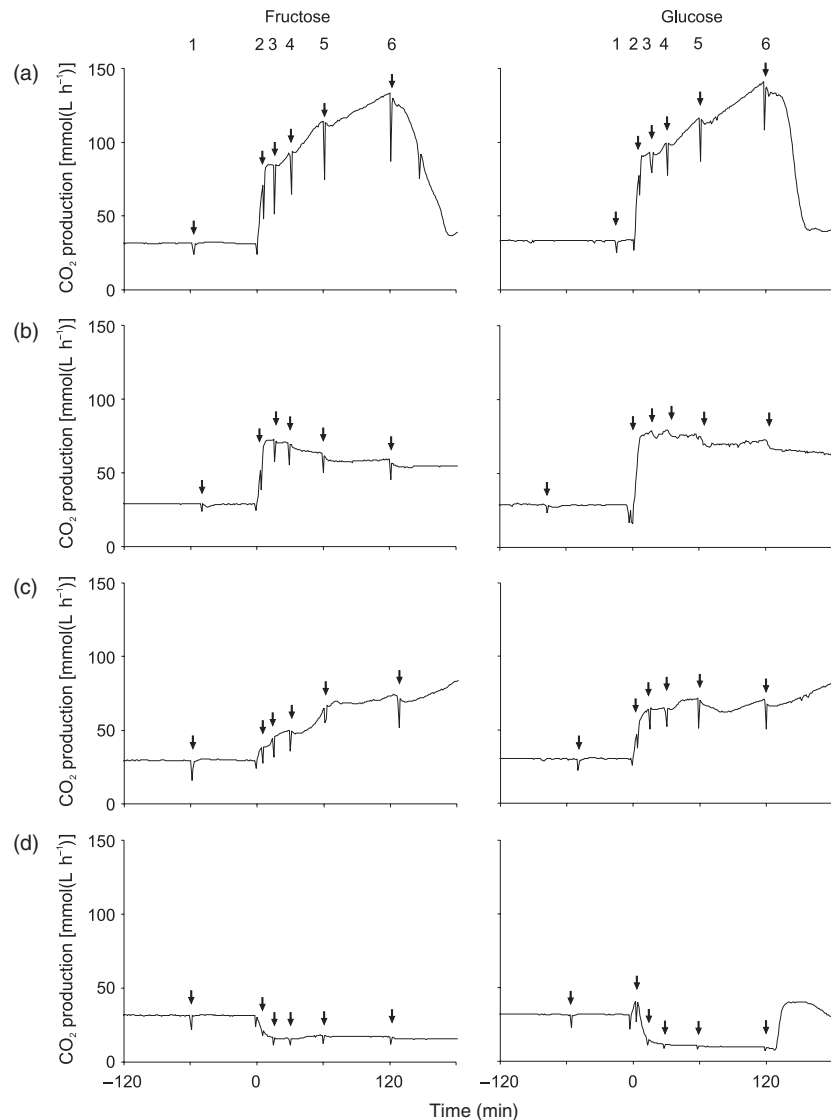


**Fig. 1.** Carbon dioxide production rate [ $\text{mmol}(\text{L reactor})^{-1} \text{min}^{-1}$ ] during aerobic growth of the (a) wild type, (b) HXT1, (c) HXT7 and (d)  $\text{TM6}^*$  strains in ethanol-limited continuous culture, with addition of sugar to a final concentration of 110 mM at time 0. The sampling points are marked with arrows and a number to facilitate identification. Arrow 1, at steady state; arrows 2–6 at 5, 15, 30, 60 and 120 min after sugar addition, respectively.

formation. This might be explained by distinct kinetics of the hexose transporters towards glucose and fructose. However, this question must be further addressed in a dedicated study (Berthels *et al.*, 2004).

### Intracellular levels of glycolytic intermediates and adenine nucleotides differed between strains with different rates of glycolysis

We chose to monitor the levels of the three first metabolites of glycolysis: G6P, F6P and F16BP, as well as adenine nucleotides, because some of these have been proposed to take part in the glucose repression response (Boles *et al.*, 1993). The most remarkable result of these measurements was the difference between the G6P and F16BP concentration of the four strains (Fig. 3c). This correlated well with the sugar consumption rate of the different strains, F16BP being high-

est in the wild type, followed, in declining order, by HXT1, HXT7 and the  $\text{TM6}^*$  strain. The opposite occurred for the levels of G6P;  $\text{TM6}^*$  exhibited the highest G6P concentration while the wild-type level was very low after sugar addition (Fig. 3a). In HXT7, the concentration of G6P changed substantially during the measured time as well as between the two sugars. The level of F6P was very low in all four strains and showed the same pattern: a rapid decrease after addition of glucose or fructose to a level close to the detection limit (Fig. 3b). It is interesting to observe that variations in G6P concentration were particularly pronounced in the  $\text{TM6}^*$  and HXT7 strains during the first 30 min after sugar addition, before stabilizing for the remaining time of the experiment. The end product of glycolysis, pyruvate, attained the highest levels in the wild type (Fig. 3d).

Large differences were observed in adenosine nucleotide levels between the  $\text{TM6}^*$  and the wild-type strains. Thus, in

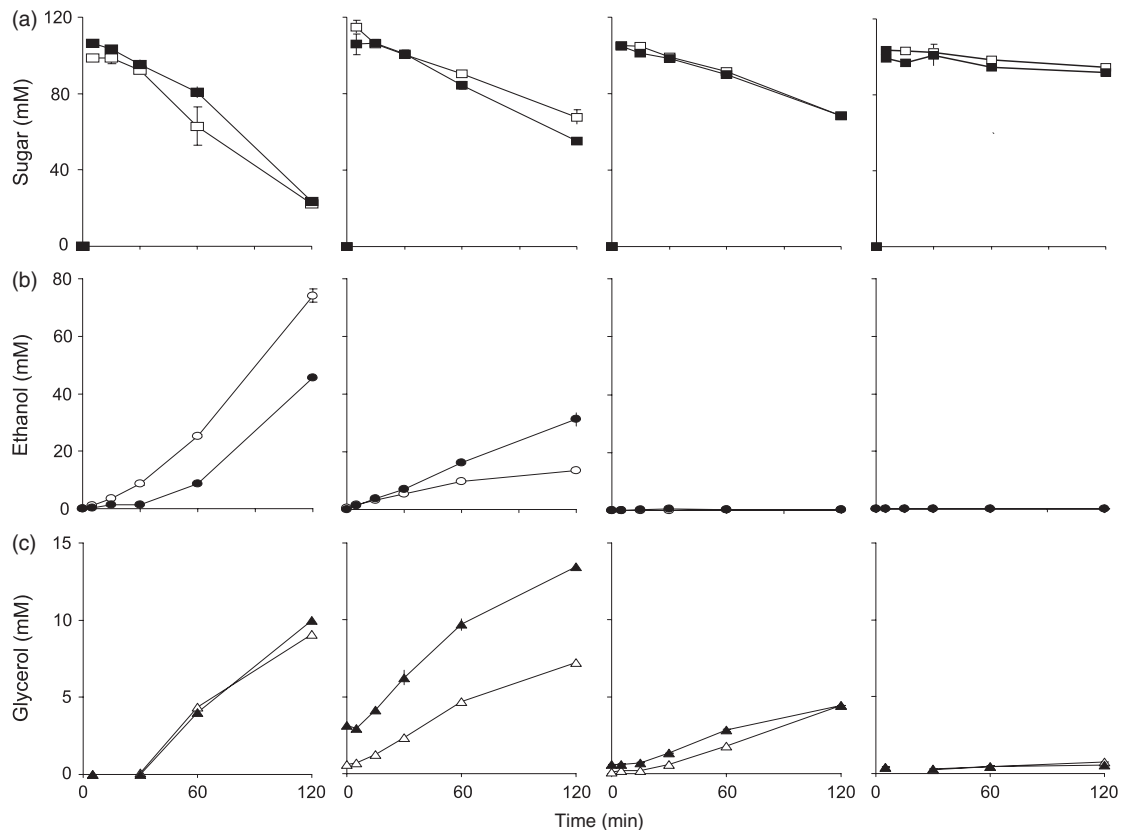


**Fig. 2.** Determination of extracellular (a) sugar (squares), (b) ethanol (circles) and (c) glycerol (triangles) after addition of glucose (filled symbols) or fructose (open symbols) to ethanol-limited chemostats. Error bars indicate the maximum and minimum values from duplicate samples.

**Table 2.** Mean sugar consumption and ethanol production rates measured over 2 h after a sugar pulse to ethanol-limited chemostats\*

Strains	Sugar consumption rate (mmol g <sup>-1</sup> h <sup>-1</sup> )		Ethanol production rate (mmol g <sup>-1</sup> h <sup>-1</sup> )	
	Fructose	Glucose	Fructose	Glucose
Wild type	3.21 ± 0.07	3.21 ± 0.03	1.76 ± 0.02	3.07 ± 0.07
HXT1	2.55 ± 0.23	2.30 ± 0.25	1.51 ± 0.13	0.63 ± 0.01
HXT7	1.48 ± 0.02	1.60 ± 0.05	0.01 ± 0.00	0.01 ± 0.01
TM6*	0.33 ± 0.03	0.42 ± 0.08	0	0

\*Glucose or fructose was added to a final concentration of 110 mM.

the mutant strain, ATP was higher (Fig. 4a), while ADP and AMP were lower (Fig. 4b and c) compared with the levels of the wild type. As a result of this, the ATP:ADP ratio as well as the ATP:AMP ratio were substantially higher in TM6\* compared with that of the wild type, while the NAD<sup>+</sup> levels remained similar in both (Fig. 4d).

#### Storage carbohydrate accumulation varied between strains with different rates of glycolysis

The TM6\*, HXT1 and HXT7 strains accumulated trehalose as well as glycogen during the ethanol-limited growth in the chemostats. The TM6\* continued to accumulate these compounds also after the sugar pulse in contrast to the

HXT1 and HXT7 strains, which, after the addition of sugar, consumed the storage carbohydrates produced earlier (Fig. 5). The short transient decrease in the trehalose content of the TM6\* strain was correlated with the small transient increase in the CO<sub>2</sub> evolution rate (Fig. 1d) during the first 15 min after the glucose pulse. The wild-type strain showed accumulation neither during ethanol-limited growth nor after the pulse, except for a transient accumulation of glycogen directly after the sugar pulse (Fig. 5).

#### Modelling of glycolytic flux control

Yeast undergoes a tremendous and rapid reprogramming in response to a sudden glucose pulse. More than 1000 genes

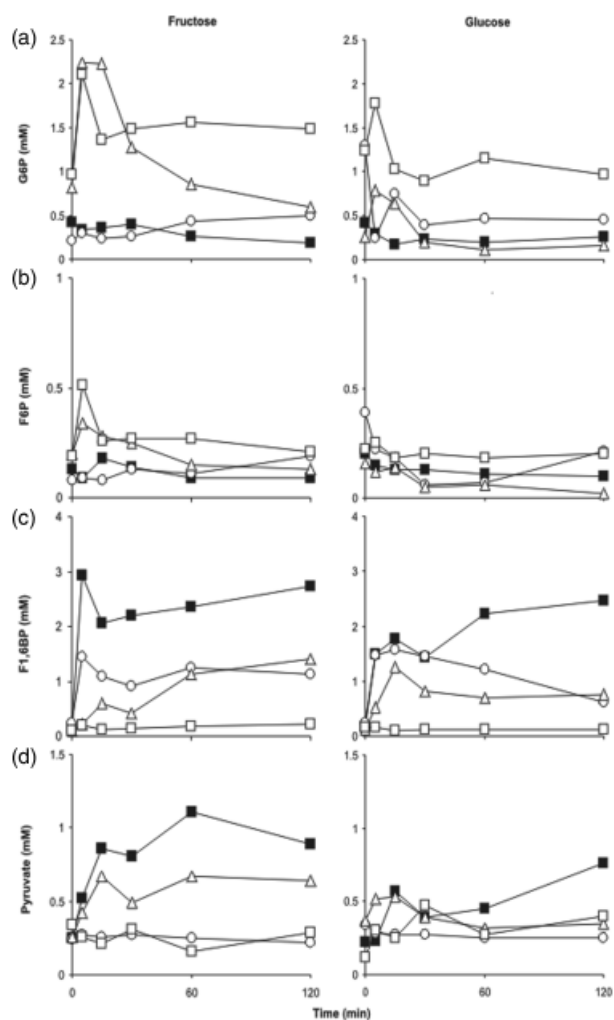


**Fig. 3.** Determination of intracellular (a) G6P, (b) F6P, (c) F16BP and (d) pyruvate, of the wild type (■), HXT1 (○), HXT7 (△) and TM6\* (□) strains. SEM was below 15% for all measurements.

were significantly affected in the first 5 min after a glucose pulse to a glucose-limited chemostat, together with significant alterations of intracellular metabolite concentrations (Kresnowati *et al.*, 2006). This initial process is still not well understood, and requires a substantially more detailed modelling approach than the one applied here. Instead, we focus on comparing the four strains during 2-h transients. During this period, metabolism is predominantly respiro-fermentative in the wild type. The model was, therefore, constructed for respiro-fermentative growth on glucose, and was not designed for detailed analysis of the short first transient from respiratory growth. The aim was to investigate whether the changes in intracellular metabolite concentrations and extracellular product profiles could be explained by shifts in enzymatic activities in the different steps of glycolysis. After parameter estimation (Table 3), the model fitted the observed trends well for most of the

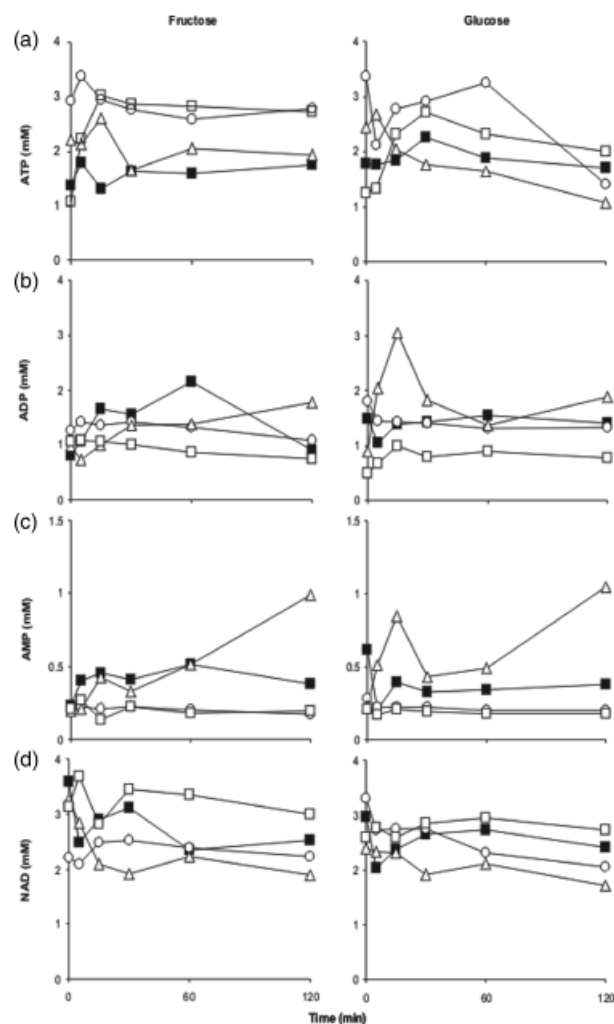


**Fig. 4.** Determination of intracellular (a) ATP, (b) ADP, (c) AMP and (d) NAD<sup>+</sup>, of the wild type (■), HXT1 (○), HXT7 (△) and TM6\* (□) strains. SEM was below 15% for all measurements.

metabolites in all four different strains (Fig. 6). The glucose uptake rate increased throughout the transients, while the hexose phosphate concentrations, with few exceptions, remained constant or decreased slightly after the first rapid changes in the early stages. This was taken into consideration by increasing the  $V_{\max}$  values of the upper part of glycolysis by a factor  $(1 + \text{Expr}_1 t)$ .

The estimated ethanol production could not be completely eliminated in the HXT7 and TM6\* strains. To reach a feasible solution for these strains, a careful balance between the maximum rates of the Lp-PDH, the PDC, the ADH and the GapDH was necessary. An imbalance led to either excessive accumulation of acetaldehyde, negative acetaldehyde concentrations or erroneous glycerol formation. Therefore, parameters were fitted by manual tuning rather than by optimization for the HXT7 and the TM6\* strains.

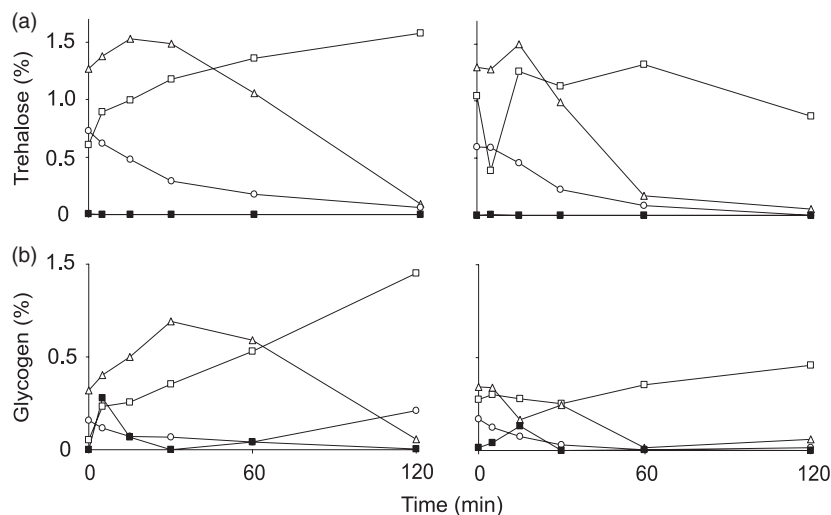


**Fig. 5.** Determination of (a) trehalose and (b) glycogen, of the wild type (■), HXT1 (○), HXT7 (△) and TM6\* (□) strains. Concentrations are expressed as percentage [g glucose released (g dry weight)<sup>-1</sup>].

The estimated initial  $V_{\max}$  of PFK decreased for all three mutant strains – from 259 mM min<sup>-1</sup> for the wild type to 9 mM min<sup>-1</sup> for the TM6\* strain (Table 3). The  $V_{\max}$  of the PGI decreased by a factor 20 in TM6\* compared with the wild type. Moreover, the rate of change of expression of the enzymes of the upper part of glycolysis was also lower in the TM6\* strain. With these parameter values, the observed differences in the concentrations of G6P, F6P and F16BP could be recreated.

To obtain reasonable values of the predicted NAD<sup>+</sup> concentrations, it was necessary to modify the sensitivity of Lp-PDH towards NAD<sup>+</sup> and NADH. This was done by including the two parameters  $K_{\text{NAD}}$  and  $K_{\text{I,NADH}}$  in the parameter optimization, in addition to the  $V_{\max}$ . The  $K_{\text{NAD}}$  and  $K_{\text{I,NADH}}$  values of the TM6\* strain were *c.* 10% and 35% of the corresponding values for the wild type strain. At constant NAD<sup>+</sup> and NADH concentrations, a lower  $K_{\text{NAD}}$  means a higher rate, but lower sensitivity to the NAD<sup>+</sup> concentration, whereas a lower  $K_{\text{I,NADH}}$  value means a lower rate but higher sensitivity to inhibition by NADH. In other words, the PDH and the TCA cycle reactions in the TM6\* strain were, as a whole, generally closer to their maximal rates, but were also more sensitive to inhibition by NADH. In the TM6\* strain, respiratory catabolism of glucose via the TCA cycle, together with a reduced growth rate, could potentially lead to an increased NADH concentration. A control structure as outlined above may, under such conditions, help to maintain the NADH levels low enough, such that any unnecessary glycerol and ethanol production is prevented.

The TM6\* strain had both a reduced glycolytic rate and a reduced growth rate during the transient. However, the TM6\* apparently had a greater energetic efficiency, because the rate constant for the nonspecific ATP consumption was only 7% of that of the wild type. Indeed, at the end of the

120-min transients, the biomass yield on ATP was much higher (22.6 g mol<sup>-1</sup>) for TM6\*, than for the wild-type strain (7.3 g mol<sup>-1</sup>). The biomass yields on ATP increased steadily for all strains, indicating a continuous adaptation to the environmental conditions.

## Discussion

In this study, four *S. cerevisiae* strains with different glycolytic rates were studied in order to understand the underlying mechanism driving the shift from respiration to fermentation. All strains were initially cultivated in aerobic chemostats, with ethanol as the only energy and carbon source. This guaranteed that all strains used a fully respiratory metabolism. When suddenly exposing the cells to a glucose (or fructose) pulse, the strains responded very differently. The wild type and the HXT1 turned immediately to a respiro-fermentative metabolism, while HXT7 and TM6\* maintained respiratory metabolism. A reduction in sugar consumption from one strain to another, such as comparing the wild type with the TM6\* strain, was accompanied by a decrease in product formation of ethanol and glycerol, accumulation of storage carbohydrates and variations in the intracellular concentrations of glycolytic metabolites and nucleotides. The intermediate consumption rates represented by the HXT1 and HXT7 strains also illustrated these trends.

In general, addition of glucose or fructose to wild-type cells triggers both glucose repression and a switch from respiratory to mainly fermentative metabolism (Rolland *et al.*, 2002). This pattern was observed for the wild-type and the HXT1 strains. Previous reports on aerobic batch cultures have shown that the ethanol production rate in the HXT7 strain is about 50% of that of the wild type (Elbing *et al.*, 2004a,b). In contrast, it was observed here that

**Table 3.** Estimated model parameter values for the wild type, HXT1, HXT7 and TM6\* strains\*

Reaction	Parameter <sup>†</sup>	Wt	HXT1	HXT7 <sup>‡</sup>	TM6* <sup>‡</sup>
HK	$V_{3m}$ (mM min <sup>-1</sup> )	1000	1000	1000	1000
PGI	$V_{4m}$ (mM min <sup>-1</sup> )	250	250	250	13
PFK	$V_{5m}$ (mM min <sup>-1</sup> )	259	71	61	9
Ald	$V_{6m}$ (mM min <sup>-1</sup> )	88	58	149	97
TPI	$V_{7m}$ (mM min <sup>-1</sup> )	116	116	116	116
GapDH	$V_{8m}$ (mM min <sup>-1</sup> )	$4.34 \times 10^6$	173	$4.1 \times 10^7$	$1.3 \times 10^5$
HKT/PGI/PFK/Ald/GapDH	Expr <sub>1</sub> (min <sup>-1</sup> )	0.06	0.05	0.06	0.004
PK	$V_{10m}$ (mM min <sup>-1</sup> )	$1.5 \times 10^5$	$1.5 \times 10^5$	$2.4 \times 10^8$	$2.4 \times 10^8$
PDC	$V_{11m}$ (mM min <sup>-1</sup> )	156	78	51	117
	Expr <sub>2</sub> (min <sup>-1</sup> )	0.20	0.09	0.29	0
ADH	$V_{12m}$ (mM min <sup>-1</sup> )	$4.12 \times 10^7$	$1.66 \times 10^{11}$	$3.7 \times 10^9$	800
Lp-GPD	$V_{15m}$ (mM min <sup>-1</sup> )	89	60	560	63
Lp-PDH	$V_m$ (mM min <sup>-1</sup> )	$4.74 \times 10^4$	$1.27 \times 10^5$	$5.0 \times 10^4$	$1.3 \times 10^3$
	$K_{NAD}$ (mM)	2170	5440	1660	250
	$K_{I,NADH}$ (mM)	4.3	5.0	22	1.5
Lp-ATP	$K_{23}$ (min <sup>-1</sup> )	122	60	50	8

\*Parameters were estimated using nonlinear least squares minimization with Gauss–Newton algorithm in MATLAB<sup>®</sup>, except where noted. Values in italics were set as constants and were not part of the optimization. See main text for further details.

<sup>†</sup>Units refer to total cell volume, mmol (L cell volume)<sup>-1</sup> min<sup>-1</sup>. The cellular volume was assumed to be 2 mL (g dry weight)<sup>-1</sup>. See Table 1 for additional parameters and notation.

<sup>‡</sup>Parameters were fitted by manual tuning. Proper optimization gave infeasible solutions.

HK, hexokinase; PGI, phosphoglucose isomerase; PFK, phosphofructokinase; Ald, aldolase; TPI, triose phosphate isomerase; GapDH, glyceraldehyde 3-phosphate dehydrogenase; Lp-PEP, lumped phosphoglycerate kinase, phosphoglycerate mutase, enolase; PK, pyruvate kinase; PDC, pyruvate decarboxylase; ADH, alcohol dehydrogenase; Lp-GPD, lumped glycerol 3-phosphate dehydrogenase and glycerol 3-phosphatase; Lp-PDH, lumped pyruvate dehydrogenase and complete TCA cycle reactions; Lp-ATP, lumped, nonspecific ATP consumption.

ethanol formation was negligible in the HXT7 strain while glycerol reached a level remarkably similar to that of the wild type. TM6\* showed fully respiratory metabolism on both glucose and fructose, in contrast to a previous study in which ethanol could be produced in substantial amounts during growth on fructose in batch culture (Henricsson *et al.*, 2005).

The different sugar consumption rates were also reflected in the concentrations of intracellular metabolites. G6P and F6P levels were higher for strains with a lower sugar consumption rate (i.e. HXT7 and TM6\*) than for those with a higher rate (i.e. wild type and HXT1). F16BP measurements produced quite the opposite result, i.e. considerably lower levels were found in the TM6\* strain compared with the wild type. A similar pattern in the enological V5.TM6\*P strain has been reported previously (Henricsson *et al.*, 2005). High concentrations of F6P and G6P, together with low levels of F16BP, may indicate that PFK activity was inhibited. Elevated G6P over F6P concentrations may indicate that the PGI activity was limited, or that the equilibrium constant was affected. Furthermore, the high degree of accumulation of carbohydrates (glycogen and trehalose) may result from an increased level of their substrate (G6P). By applying the kinetic model of the central metabolic fluxes, it was found that alterations in the maximal rates of PFK and PGI could indeed explain the

metabolite concentrations measured for the different strains. The simulations also reproduced the high levels of ATP in the TM6\* strain. Under these conditions, ATP acts as a powerful inhibitor of PFK, without being counteracted by AMP (Reibstein *et al.*, 1986; Sols *et al.*, 1989; Larsson *et al.*, 2000). Another well-known regulator of PFK activity is F26BP, whose synthesis and degradation is regulated by cAMP-activated protein kinases (Heinisch *et al.*, 1996). Cells growing on respiratory carbon sources are known to exhibit a transient increase in cAMP levels on addition of glucose (Rolland *et al.*, 2001). F26BP was not measured, and its effect on PFK could thus only be included via an assumed constant concentration based on the literature data. Although adenylate cyclase, the enzyme responsible for synthesis of cAMP from ATP, is activated by one branch responding to external glucose concentrations (Gpr1), there is another branch that requires glucose, fructose or mannose phosphorylation (Ras). The latter could be impaired in strains with reduced sugar uptake, therefore leading to abnormally low levels of cAMP. This view is supported by the high levels of glycogen and trehalose observed in this experiment, compared with the wild type.

The total pool of adenine nucleotide as well as the individual nucleotides undergo rapid transients during the first 5 min of a glucose pulse, in part due to the massive transcriptional reprogramming and protein synthesis

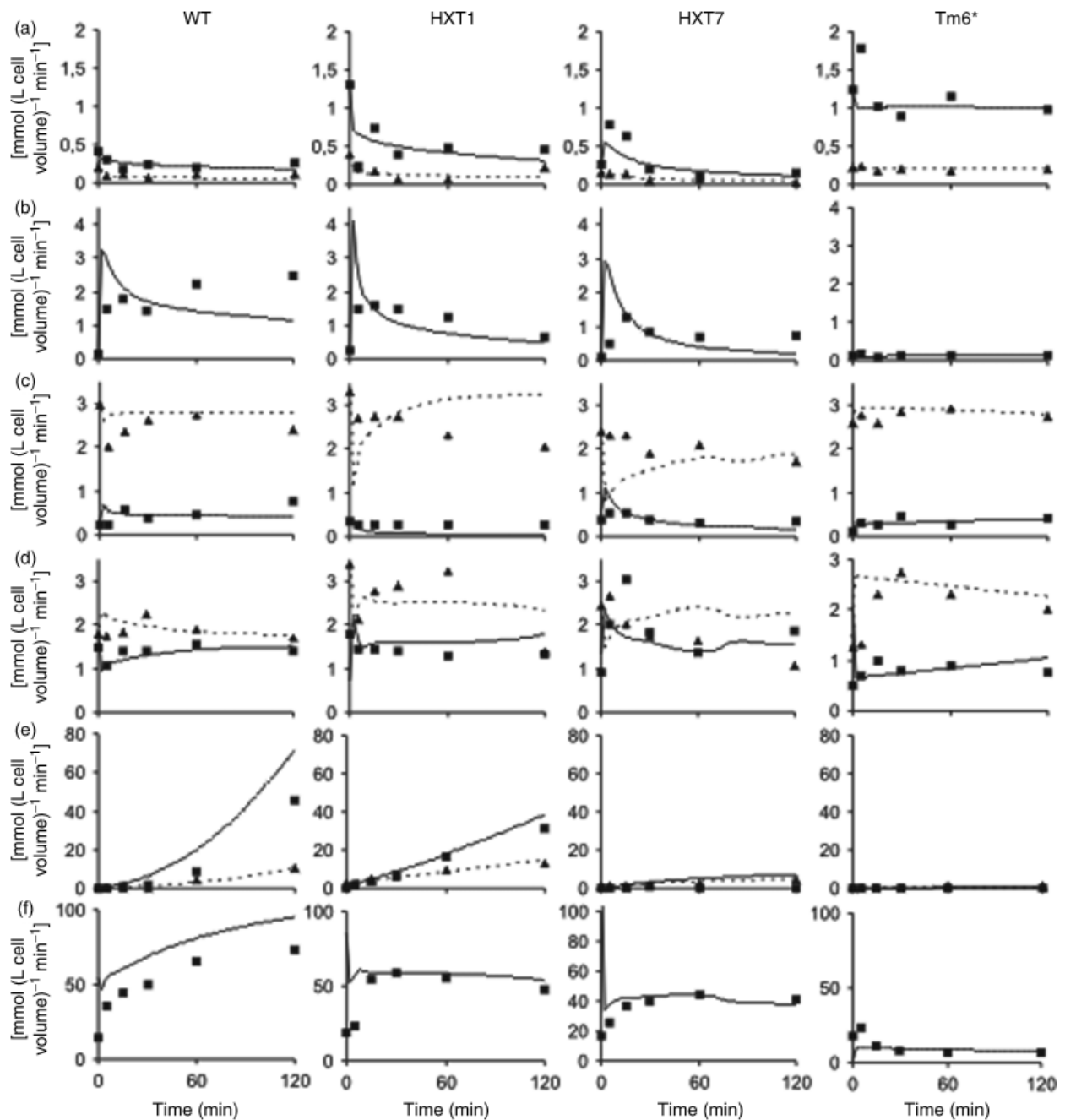


**Fig. 6.** Simulation of intracellular metabolite concentrations compared with experimental data. (a) G6P (squares, solid line) and F6P (triangles, dashed line), (b) F16BP, (c), pyruvate (squares, solid line) and  $\text{NAD}^+$  (triangles, dashed line) (d) ADP (squares, solid line) and ATP (triangles, dashed line) (e) extracellular ethanol (squares, solid line) and glycerol (triangles, dashed line) and (f)  $\text{CO}_2$  production rate [ $\text{mmol (L cell volume)}^{-1} \text{min}^{-1}$ ]. Symbols denote experimental data and lines indicate simulated values.

(Kresnowati *et al.*, 2006). During the 120 min duration of the experiments, the size and distribution of the AxP pool continue to change. The ATP:AMP ratio is a potential candidate for the initial glucose repression signal, because it links energy availability and sugar degradation; in addition, it is known to have regulatory functions on sensing compo-

nents of mammalian cells, particularly on the AMP-activated protein kinase (AMPK) (Wilson *et al.*, 1996). However, attempts to explain glycolytic regulation in yeast according to low energetic levels have found limited support (Hardie *et al.*, 1998) particularly because Snf1, the yeast homologue of AMPK (Celenza & Carlson, 1986; Hardie

*et al.*, 1998), does not respond to ATP or AMP *in vitro*. One hypothesis would be that the ATP:AMP ratio acts as a primary signal on glycolytic enzymes, e.g. PFK, HK and PK and the outcome affects one or several glucose responsive signalling networks such as, for example, Snf1. Nevertheless, it was found that the ATP:AMP ratio displayed in TM6\* was considerably higher than that in the wild type. This could be the result of either a higher energetic efficiency (P/O ratio) or a lower nonspecific ATP consumption of the TM6\* strain compared with the wild type. From the results, we cannot distinguish between these, but the effect is manifest in the lower estimated rate constant for the nonspecific ATP consumption, and in the higher biomass yield on ATP. Following up the same line of correlations as in mammals, the higher ATP:AMP ratio should result in an inactive Snf1. In contrast, it has indeed been shown that Snf1 is active in TM6\* consistent with a glucose-derepressed strain (Elbing *et al.*, 2004b). The conclusion is that a direct correlation between the ATP:AMP ratio and Snf1 activity does not apply, at least not in explaining the derepressed state of the TM6\* strain at high external glucose concentrations.

Earlier evidence has been presented (Elbing *et al.*, 2004a) that the dominating control on the glycolytic flux in TM6\* was exerted by the limited uptake capacity of the hexose transporter (the Tm6\* protein). This resulted in the respiratory phenotype of the TM6\* strain. However, in the former study, strains were grown in batch cultures with glucose as the only carbon and energy source. In this study, on the other hand, measurements of uptake capacity of the four strains were retrieved during steady-state growth on ethanol. In this case, the uptake capacity did not show any substantial difference between the strains. Still, the cells showed large differences in response to sugar addition, both concerning the immediate response and the response registered 2 h after sugar addition. These new data complement the earlier presented hypothesis from the authors' laboratory, which pinpoints the hexose transport ability of the TM6\* strain as the main controlling agent of its respiratory phenotype (Elbing *et al.*, 2004a). The present study illustrates that the main controlling mechanism may differ depending on the cultivation conditions under which cells are grown. PFK has for a long time been regarded as a key enzyme in the regulation of the glycolytic rate; however, in recent years, it has been proposed that its main role would be played during carbon-source adaptation (Heinisch *et al.*, 1996; Rodicio *et al.*, 2000). In line with this hypothesis, we show that changed kinetics of PGI and PFK, and a modified sensitivity of PDH and the TCA cycle towards NAD<sup>+</sup> and NADH, may be responsible for the shift from respiro-fermentative to respiratory metabolism. The present data are not sufficient to derive the mechanisms underlying these kinetic modifications.

The initial glucose repression signal remains elusive and further work will have to be performed to identify its nature. We believe that the set of strains used in this study will contribute to disclosing the mechanism of glucose repression in yeast, for instance by studying the transcriptional response after addition of glucose. On the other hand, this study has contributed with novel information on the control of the regulation between respiro-fermentative and respiratory metabolism.

## Acknowledgements

This work was supported by grants from the Swedish Research Council (621-2004-3550) and the National Research School for Genomics and Bioinformatics. The authors gratefully acknowledge Fitri Hadiyah for the initial modelling work, and Karin Elbing and Elisabeth Thomsson for fruitful discussions.

## Authors' contribution

D.B. and M.J. contributed equally to this work.

## References

- Albers E, Larsson C, Lidén G, Niklasson C & Gustafsson L (1996) Influence of the nitrogen source on *Saccharomyces cerevisiae* anaerobic growth and product formation. *Appl Environ Microbiol* **62**: 3187–3195.
- Berthels NJ, Cordero Otero RR, Bauer FF, Thevelein JM & Pretorius IS (2004) Discrepancy in glucose and fructose utilisation during fermentation by *Saccharomyces cerevisiae* wine yeast strains. *FEMS Yeast Res* **4**: 683–689.
- Boles E & Hollenberg CP (1997) The molecular genetics of hexose transport in yeast. *FEMS Microbiol Rev* **21**: 85–111.
- Boles E & Zimmermann FK (1993) Induction of pyruvate decarboxylase in glycolysis mutants of *Saccharomyces cerevisiae* correlates with the concentrations of three-carbon glycolytic metabolites. *Arch Microbiol* **160**: 324–328.
- Boles E, Zimmermann FK & Heinisch J (1993) Different signals control the activation of glycolysis in the yeast *Saccharomyces cerevisiae*. *Yeast* **9**: 761–770.
- Boles E, Zimmermann FK & Thevelein JM (1997) Metabolic signals. *Yeast Sugar Metabolism* (Zimmermann FK & Entian K-D, eds), pp. 379–408. Technomic Publishing Co, Lancaster.
- Carlson M (1999) Glucose repression in yeast. *Curr Opin Microbiol* **2**: 202–207.
- Celenza JL & Carlson M (1986) A yeast gene that is essential for release from glucose repression encodes a protein kinase. *Science* **233**: 1175–1180.
- Cho Y-H, Yoo S-D & Sheen J (2006) Regulatory functions of nuclear hexokinase1 complex in glucose signaling. *Cell* **127**: 579–589.

- de la Cera T, Herrero P, Moreno-Herrero F, Chaves RS & Moreno F (2002) Mediator factor Med8p interacts with the hexokinase 2: implication in the glucose signalling pathway of *Saccharomyces cerevisiae*. *J Mol Biol* **319**: 703–714.
- DeRisi JL, Iyer VR & Brown PO (1997) Exploring the metabolic and genetic control of gene expression on a genomic scale. *Science* **278**: 680–686.
- De Winde J, Crauwels M, Hohmann S, Thevelein J & Winderickx J (1996) Differential requirement of the yeast sugar kinases for sugar sensing in establishing the catabolite-repressed state. *Eur J Biochem* **241**: 633–643.
- Dihazi H, Kessler R & Eschrich K (2004) High osmolarity glycerol (HOG) pathway-induced phosphorylation and activation of 6-phosphofructo-2-kinase are essential for glycerol accumulation and yeast cell proliferation under hyperosmotic stress. *J Biol Chem* **279**: 23961–23968.
- Elbing K, Larsson C, Bill RM, Albers E, Snoep JL, Boles E, Hohmann S & Gustafsson L (2004a) Role of hexose transport in control of glycolytic flux in *Saccharomyces cerevisiae*. *Appl Environ Microbiol* **70**: 5323–5330.
- Elbing K, Ståhlberg A, Hohmann S & Gustafsson L (2004b) Transcriptional responses to glucose at different glycolytic rates in *Saccharomyces cerevisiae*. *Eur J Biochem* **271**: 4855–4864.
- Fiechter A, Fuhrmann GF & Kappeli O (1981) Regulation of glucose metabolism in growing yeast cells. *Adv Microb Physiol* **22**: 123–183.
- Gancedo JM (1998) Yeast carbon catabolite repression. *Microbiol Mol Biol Rev* **62**: 334–361.
- Ganzhorn AJ, Green DW, Hershey AD, Gould RM & Plapp BV (1987) Kinetic characterization of yeast alcohol dehydrogenases. Amino acid residue 294 and substrate specificity. *J Biol Chem* **262**: 3754–3761.
- Gustafsson L (1979) The ATP pool in relation to the production of glycerol and heat during growth of the halotolerant yeast *Debaryomyces hansenii*. *Arch Microbiol* **120**: 15–23.
- Hardie DG, Carling D & Carlson M (1998) The AMP-activated/SNF1 protein kinase subfamily: metabolic sensors of the eukaryotic cell? *Annu Rev Biochem* **67**: 821–855.
- Heinisch JJ, Boles E & Timpel C (1996) A yeast phosphofructokinase insensitive to the allosteric activator fructose 2,6-bisphosphate. Glycolysis/metabolic regulation/allosteric control. *J Biol Chem* **271**: 15928–15933.
- Henricsson C, de Jesus Ferreira MC, Hedfalk K, Elbing K, Larsson C, Bill RM, Norbeck J, Hohmann S & Gustafsson L (2005) Engineering of a novel *Saccharomyces cerevisiae* wine strain with a respiratory phenotype at high external glucose concentrations. *Appl Environ Microbiol* **71**: 6185–6192.
- Hohmann S, Winderickx J, de Winde J, Valckx D, Cobbaert P, Luyten K, de Meirsmen C, Ramos J & Thevelein J (1999) Novel alleles of yeast hexokinase PII with distinct effects on catalytic activity and catabolite repression of *SUC2*. *Microbiology* **145**: 703–714.
- Hynne F, Danø S & Sørensen PG (2001) Full-scale model of glycolysis in *Saccharomyces cerevisiae*. *Biophys Chem* **94**: 121–163.
- Johannes KJ & Hess B (1973) Allosteric kinetics of pyruvate kinase of *Saccharomyces carlsbergensis*. *J Mol Biol* **76**: 181–205.
- Kresnowati MTAP, van Winden WA, Almering MJH, ten Pierick A, Ras C, Knijnenburg TA, Daran-Lapujade P, Pronk JT, Heijnen JJ & Daran JM (2006) When transcriptome meets metabolome: fast cellular responses of yeast to sudden relief of glucose limitation. *Mol Syst Biol* **2**: 1–16.
- Larsson C, Pålman I-L & Gustafsson L (2000) The importance of ATP as a regulator of glycolytic flux in *Saccharomyces cerevisiae*. *Yeast* **16**: 797–809.
- Mojžita D (2007) Thiamine-related regulation of metabolism and gene expression in the yeast *Saccharomyces cerevisiae*. PhD Thesis, Göteborg University, Göteborg, Sweden.
- Mounolou J (1975) The properties and composition of yeast nucleic acids. *The Yeasts* (Rose AH & Harrison JS, eds), pp. 309–334. Academic Press, London.
- Otterstedt K, Larsson C, Bill R, Ståhlberg A, Boles E, Hohmann S & Gustafsson L (2004) Switching the mode of metabolism in the yeast *Saccharomyces cerevisiae*. *EMBO Rep* **5**: 1–6.
- Özcan S & Johnston M (1999) Function and regulation of yeast hexose transporters. *Microbiol Mol Biol Rev* **63**: 554–559.
- Özcan S, Freidel K, Leuker A & Ciriacy M (1993) Glucose uptake and catabolite repression in dominant *HTR1* mutants of *Saccharomyces cerevisiae*. *J Bacteriol* **175**: 5520–5528.
- Parrou JL & François J (1997) A simplified procedure for a rapid and reliable assay of both glycogen and trehalose in whole yeast cells. *Anal Biochem* **248**: 186–188.
- Postma E, Scheffers WA & van Dijken JP (1989) Kinetics of growth and glucose transport in glucose-limited chemostat cultures of *Saccharomyces cerevisiae* CBS 8066. *Yeast* **5**: 159–165.
- Regelmann J, Schule T, Josupeit FS, Horak J, Rose M, Entian KD, Thumm M & Wolf DH (2003) Catabolite degradation of fructose-1,6-bisphosphatase in the yeast *Saccharomyces cerevisiae*: a genome-wide screen identifies eight novel *GID* genes and indicates the existence of two degradation pathways. *Mol Biol Cell* **14**: 1652–1663.
- Reibstein D, den Hollander JA, Pilkis SJ & Shulman RG (1986) Studies on the regulation of yeast phosphofructo-1-kinase: its role in aerobic and anaerobic glycolysis. *Biochemistry (Moscow)* **25**: 219–227.
- Rizzi M, Baltés M, Theobald U & Reuss M (1997) *In vivo* analysis of metabolic dynamics in *Saccharomyces cerevisiae*: II. Mathematical model. *Biotechnol Bioeng* **55**: 592–608.
- Rodicio R, Strauss A & Heinisch JJ (2000) Single point mutations in either gene encoding the subunits of the heterooctameric yeast phosphofructokinase abolish allosteric inhibition by ATP. *J Biol Chem* **275**: 40952–40960.
- Rolland F, Winderickx J & Thevelein J (2001) Glucose-sensing mechanism in eukaryotic cells. *Trends Biochem Sci* **26**: 310–317.

- Rolland F, Winderickx J & Thevelein J (2002) Glucose-sensing and -signalling mechanisms in yeast. *FEMS Yeast Res* **2**: 183–201.
- Ronne H (1995) Glucose repression in fungi. *Trends Genet* **11**: 12–17.
- Rose M, Albig W & Entian K (1991) Glucose repression in *Saccharomyces cerevisiae* is directly associated with hexose phosphorylation by hexokinases PI and PII. *Eur J Biochem* **199**: 511–518.
- Sárvári Horváth I, Franzén CJ, Taherzadeh MJ, Niklasson C & Lidén G (2003) Effects of furfural on the respiratory metabolism of *Saccharomyces cerevisiae* in glucose-limited chemostats. *Appl Environ Microbiol* **69**: 4076–4086.
- Sols A, Gancedo C & De la Fuente G (1989) Energy-yielding metabolism. *The Yeast* (Rose H & Harrison J, eds), pp. 271–307. Academic Press, New York.
- Teusink B, Passarge J, Reijenga CA, Esgalhado E, van der Weijden CC, Schepper M, Walsh MC, Bakker BM, van Dam K, Westerhoff HV & Snoep JL (2000) Can yeast glycolysis be understood in terms of *in vitro* kinetics of the constituent enzymes? Testing biochemistry. *Eur J Biochem* **267**: 5313–5329.
- van Dijken JP, Bauer J, Brambilla L *et al.* (2000) An interlaboratory comparison of physiological and genetic properties of four *Saccharomyces cerevisiae* strains. *Enzyme Microb Technol* **26**: 706–714.
- Verduyn C, Zomerdijk T, Van Dijken JP & Scheffers WA (1984) Continuous measurement of ethanol production by aerobic yeast suspensions with an enzyme. *Appl Microbiol Biotechnol* **19**: 181–185.
- Verduyn C, Postma E, Scheffers WA & Dijken JPV (1992) Effect of benzoic acid on metabolic fluxes in yeasts: a continuous-culture study on the regulation of respiration and alcoholic fermentation. *Yeast* **8**: 501–517.
- Walsh MC, Smits HP, Scholte M & van Dam K (1994) Affinity of glucose transport in *Saccharomyces cerevisiae* is modulated during growth on glucose. *J Bacteriol* **176**: 953–958.
- Wieczorke R, Krampe S, Weierstall T, Freidel K, Hollenberg CP & Boles E (1999) Concurrent knock-out of at least 20 transporter genes is required to block uptake of hexoses in *Saccharomyces cerevisiae*. *FEBS Lett* **464**: 123–128.
- Wilson WA, Hawley SA & Hardie DG (1996) Glucose repression/derepression in budding yeast: SNF1 protein kinase is activated by phosphorylation under derepressing conditions, and this correlates with a high AMP : ATP ratio. *Curr Biol* **6**: 1426–1434.